

A SEASONAL INVESTIGATION ON LAND SURFACE TEMPERATURE AND SPECTRAL INDICES IN IMPHAL CITY, INDIA

ANUPAM PANDEY^A, ARUN MONDAL^B, SUBHANIL GUHA^{C*},
PRADEEP KUMAR UPADHYAY^A, RASHMI^A

^a*Department of Geography, University of Allahabad, Prayagraj, Uttar Pradesh, India*

^b*School of Earth, Ocean and Environment, University of South Carolina, Columbia, SC, USA*

^c*Department of Applied Geology, National Institute of Technology Raipur, Chhattisgarh, India*

*Corresponding author email: subhanilguha@gmail.com

Received: 5th August 2022, **Accepted:** 14th September 2022

ABSTRACT

The study focused on investigating the seasonal and spatiotemporal relationship between the relationships of LST with four spectral indices (MNDWI, NDBaI, NDBI, and NDVI) in and around Manipur City of India using eight cloud-free Landsat data from the summer and winter seasons for 1991, 2001, 2011, and 2021. These spectral indices respond differently to the change of LST in an urban landscape. Pearson's linear correlation coefficient was the basis of the correlation analysis. The study finds that LST builds a moderate negative relationship with NDVI ($R = -0.42$) and MNDWI ($R = -0.42$), a moderate positive relationship with NDBaI ($R=0.48$), and NDBI ($R = 0.61$). The relationship is more stable in the winter season (CV = 7.31, 7.04, 10.45, and 28.71 for MNDWI, NDBaI, NDBI, and NDVI, respectively) than in summer (CV = 44.46, 36.09, 23.67, and 29.71 for MNDWI, NDBaI, NDBI, and NDVI, respectively). The strength of the relationship is gradually increasing in the winter season while there is no such effect noticed on the trend in the summer season. The LST-NDBI relationship is the most consistent (CV = 18.19), while the LST-NDVI relationship is the most variable (CV = 30.37).

Keywords: Imphal city; LST; MNDWI; NDBaI; NDBI; NDVI.

INTRODUCTION

Nowadays, land surface temperature (LST) estimation is considered the most important task in the study of thermal infrared remote sensing where the thermal status of varying land use/land cover (LULC) may control the generation of heat island effect in mixed urban landscapes (Arnfield, 2003; Rizwan *et al.*, 2008; Rinner & M. Hussain, 2011; Mirzaei, 2015; Zhao *et al.*, 2016). Various spectral indices based on different bands of satellite images were applied in LST-related research to evaluate the changing orientation of LST in various types of physical and cultural landscapes (Li *et al.*, 2011; Song *et al.*, 2014; Peng *et al.*, 2016). Some new relevant articles described statistical methods between LST and spectral indexes in different cities (Feyisa *et al.*, 2016; Nie *et al.*, 2016; Deilami & Kamruzzaman, 2017; Lopez *et al.*, 2017; Pearsall, 2017).

Currently, the relationships between LST and various normalized difference spectral indices were constructed using thermal infrared remote sensing; e.g., the LST-NDVI relationship (Ferelli *et al.*, 2018; Jamei *et al.*, 2019); LST-MNDWI relationship (Guha & Govil, 2021; Taripanah & Ranjbar, 2021); LST-NDBI relationship (Feng *et al.*, 2018; Filho *et al.*, 2019; Son *et al.*, 2020); LST-NDBaI relationship (Chen & Zhang, 2017; Equere *et al.*, 2020; Nimish *et al.*, 2020). However, a seasonal analysis of the LST-spectral index relation in northeast India is rare.

It is very essential to build the LST-spectral index relationship for sustainable urban planning. The positive value of each index extracts a particular type of land surface material. The land surface material influences the rise or fall of LST in a certain area. These spectral indices were generated by using different spectral bands of remotely-sensed data. They respond differently to different land use patterns. LST depends heavily on various types of landscapes. Built-up areas, dry soil, rocks, metalled roads, and concrete infrastructure enhance the value of LST whereas water, wetland, forest, grassland, scrubland, and cultivated land reduce the LST value. The health and coverage of these various types of landscape structures vary in every season. Consequently, the strength of these LST-spectral indices relationships can change seasonally.

Thus, to evaluate the specific features of seasonal variation of LST-spectral indices correlation in a mixed urban area, Imphal city was selected as it is not influenced by harsh environmental conditions and is a fast-growing city. Imphal of Manipur is an important and emerging multifunctional city in northeast India. It consists of a large percentage of forest-covered areas inside and the surroundings of the city. Available research works on Imphal city are rare. Kalota (2016) retrieved the surface temperature of the whole Manipur State by using some physical and cultural variables. Mondal *et al.* (2021) identified the urban heat island zones of Imphal and focused on its ecological status. The present study analyses the nature, strength, and trend of the effect of LST on NDVI, MNDWI, NDBI, and NDBaI in the summer and winter seasons with a gap of ten years. This work is very helpful for land use planners and environmentalists because each of these indices can identify a special type of land use (e.g., MNDWI for water bodies, NDBaI for bare land, NDBI for built-up surface, and NDVI for green vegetation) on which the LST varies significantly (Guha *et al.* 2017). The primary objectives of the research are (i) to find out the seasonal values of LST and the four indices of the study area for the study span; and (ii) to investigate the seasonal status of the spectral indices-LST relationship.

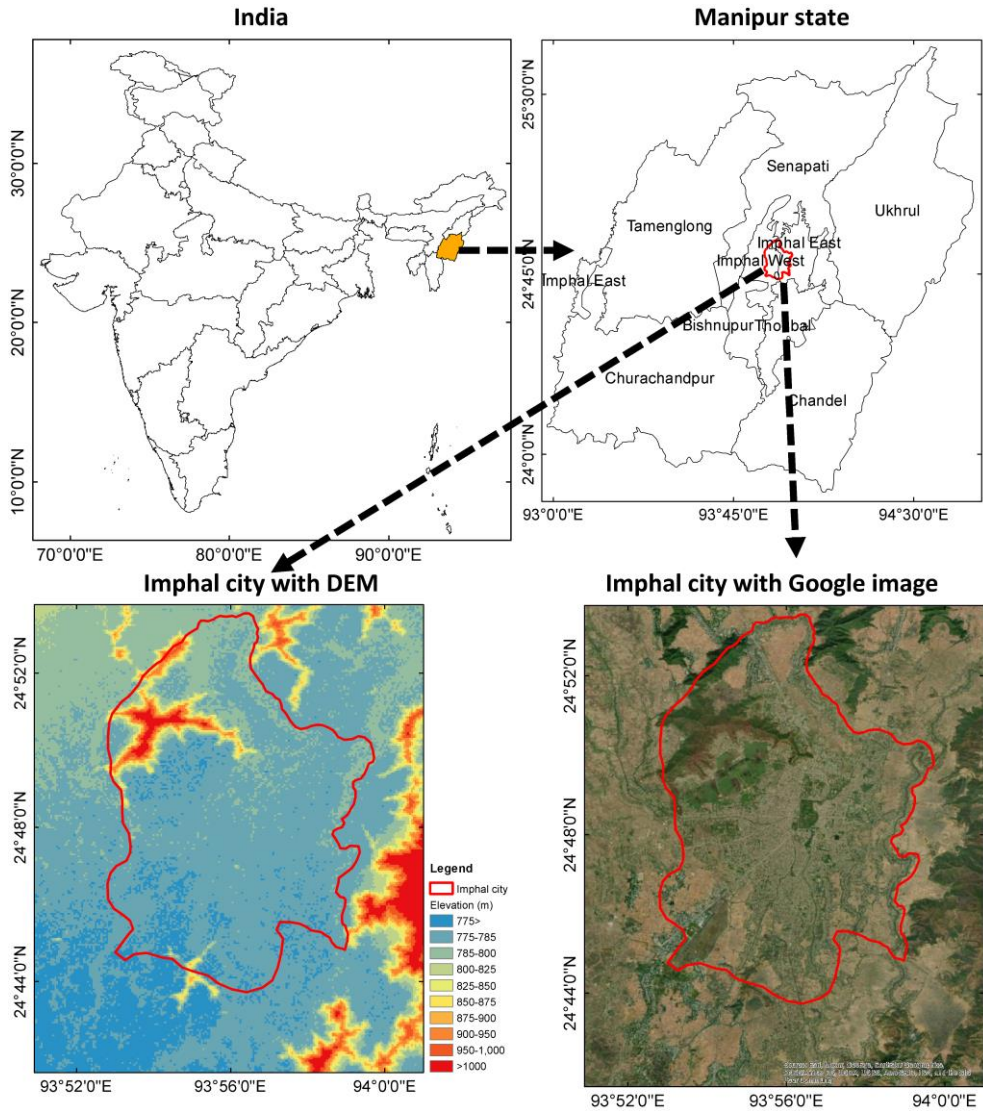
MATERIAL AND METHODS

Study area

Imphal city and the adjacent region was the selected area for the present research activities. The study area extends from 24°53'47"N to 24°41'43"N and from 93°51'00"E to 94°01'00"E (Figure 1) and it roughly covers an area of 420 km². The average elevation of the area is more than 780 m. The elevation is quite high (>900 m) in the northwest part whereas it is low (<800 m) in the southern portion. Imphal and Nambul are the two major rivers in the study area. The city has a humid subtropical climate where winter is cool and dry while the summer remains hot and wet. Imphal city experiences the summer season from April until August. During winter (November to February), the weather remains cool, comfortable, enjoyable, and characterized by a clear sky. The average maximum temperature of the summer months is around 29° C whereas the average minimum temperature of the winter months is around 5° C. The mean annual temperature is around 20° C and the mean annual rainfall is

145 cm. The soil of the study area is alluvial and it is slightly acidic. The main forest types are tropical wet evergreen, tropical moist deciduous, montane wet temperate, and sub-tropical pine. It is a famous tourist place in northeast India. Keibul Lamjao National Park is an important tourist spot. The total population of the city was 268,243 according to the 2011 census report.

Fig. 1: The study area (SRTM DEM image and Google image)



Data

Table 1: Specification of the used Landsat satellite images

Landsat scene ID	Date of acquisition	Coordinated universal time (UTC)	Path/Row	Sun elevation (°)	Sun azimuth (°)	Cloud cover (%)	Earth-Sun distance (astronomical unit)	Resolution of VNIR bands (m)	Resolution of TIR bands (m)
Summer season									
LT51350431991108BKT00	18-Apr-91	03:34:00	135/043	56.09	108.42	7.00	1.00	30	120
LT51350432001135BKT01	15-May-01	03:52:12	135/043	64.13	97.29	5.00	1.01	30	120
LT51350432011099BKT01	09-Apr-11	04:01:51	135/043	59.68	119.96	0.00	1.00	30	120
LC81350432021110LGN00	20-Apr-21	04:11:42	135/043	64.64	116.66	9.64	1.00	30	100
Winter season									
LT51350431991028ISP00	28-Jan-91	03:32:37	135/043	34.42	137.09	1.00	0.98	30	120
LT51350432001039BKT00	08-Feb-01	03:52:05	135/043	39.76	138.59	0.00	0.99	30	120
LT51350432011035BKT00	04-Feb-11	04:02:01	135/043	40.21	142.28	0.00	0.99	30	120
LC81350432021014LGN00	14-Jan-21	04:12:14	135/043	37.97	149.60	7.94	0.98	30	100

To analyse the relationship of LST with spectral indices Landsat data is selected as the sensor provides the thermal band of 100 m or 120 m spatial resolution every sixteen days intervals and this data is freely downloadable. Eight (two each from 1991, 2001, 2011, and 2021) almost cloud-free (<10 % cloud coverage) Landsat satellite imageries of Imphal city were taken from the United States Geological Survey (<http://earthexplorer.usgs.gov/>) that are used in this study (Table 1). Red and near-infrared (NIR) bands were used to determine the NDVI and the thermal infrared (TIR) band was used to estimate the LST. Shuttle Radar Topographic Mission (SRTM) Digital Elevation Model (DEM) data (<http://earthexplorer.usgs.gov/>) with 30 m spatial resolution was also used to determine the surface elevation. Imphal Municipal Corporation (<https://imc.mn.gov.in/>) provides spatial information about the city. Moreover, the Google Earth Image (<https://earth.google.com/web/>) verifies the classified images of various LULC types. The entire research work has been processed in ERDAS Imagine and ArcGIS software.

Description of the spectral indices

The study aims to investigate the seasonal and spatiotemporal changes of LST, NDVI, MNDWI, NDBI, and NDBaI in the study area from 1991 to 2021. Besides, the relationships between the spectral indices with the LST have also been determined. The whole study has been conducted during the summer and winter seasons. NIR and Red bands are used to determine NDVI. MNDWI is computed by using the Green and SWIR1 bands. SWIR1 and NIR bands are used to determine NDBI. SWIR1 and TIR bands are required to calculate NDBaI. Moreover, the TIR band is used with the Red and NIR bands to estimate the land surface emissivity and LST. After finding the spectral indices and LST of all eight images (summer and winter images for 1991, 2001, 2011, and 2021), the relationship of the individual spectral index with LST has been determined for each image.

Various types of spectral indices extract different types of LULC. The major LULC types in the urban land are green vegetation, water, wetland, barren land, and settlement. Thus, MNDWI (Xu 2006), NDBaI (Zhao & Chen, 2005), NDVI (Tucker, 1979), and NDBI (Zha *et al.*, 2003) were the chosen spectral indices as these can extract water body, bare land, settlement, and vegetation by applying their numerical thresholds (Chen *et al.*, 2006). These four indices (Table 2) were used for seasonal investigation of the relationship with LST.

Table 2: A detail description of four spectral indices

Acronym	Description	Formulation	References
NDVI	Normalized difference vegetation index	NIR-Red/NIR+Red	Tucker 1979
MNDWI	Modified normalized difference water index	Green-SWIR1/Green+SWIR1	Xu 2006
NDBI	Normalized difference built-up index	SWIR1-NIR/SWIR1+NIR	Zha et al. 2003
NDBaI	Normalized difference bareness index	SWIR1-TIR/SWIR1+TIR	Zhao and Chen 2005

LST estimation

LST computation by using Landsat TIR band follows some sequential algorithms. First, spectral radiance is calculated by Eq. 1 (Artis & Carnahan, 1982):

$$L_{\lambda} = \text{RadianceMultiBand} \times DN + \text{RadianceAddBand} \quad (1)$$

L_{λ} = the spectral radiance in $\text{Wm}^{-2}\text{sr}^{-1}\text{mm}^{-1}$.

After that, at-sensor brightness temperature is estimated by Eq. 2:

$$T_B = \frac{K_2}{\ln((K_1/L_{\lambda})+1)} \quad (2)$$

Where, T_B = brightness temperature in Kelvin (K), L_{λ} = spectral radiance in $\text{Wm}^{-2}\text{sr}^{-1}\text{mm}^{-1}$; K_2 and K_1 = calibration constants.

Thereafter, fractional vegetation is computed by Eq. 3 (Carlson & Ripley, 1997).

$$F_v = \left(\frac{NDVI - NDVI_{min}}{NDVI_{max} - NDVI_{min}} \right)^2 \quad (3)$$

Where, $NDVI_{min}$ = minimum NDVI, $NDVI_{max}$ = maximum NDVI. F_v = fractional vegetation.

Next, land surface emissivity \mathcal{E} , is computed by Eq. 4 (Sobrino *et al.*, 2001; 2004):

$$\mathcal{E} = 0.004 * F_v + 0.986 \quad (4)$$

Where, \mathcal{E} = surface emissivity.

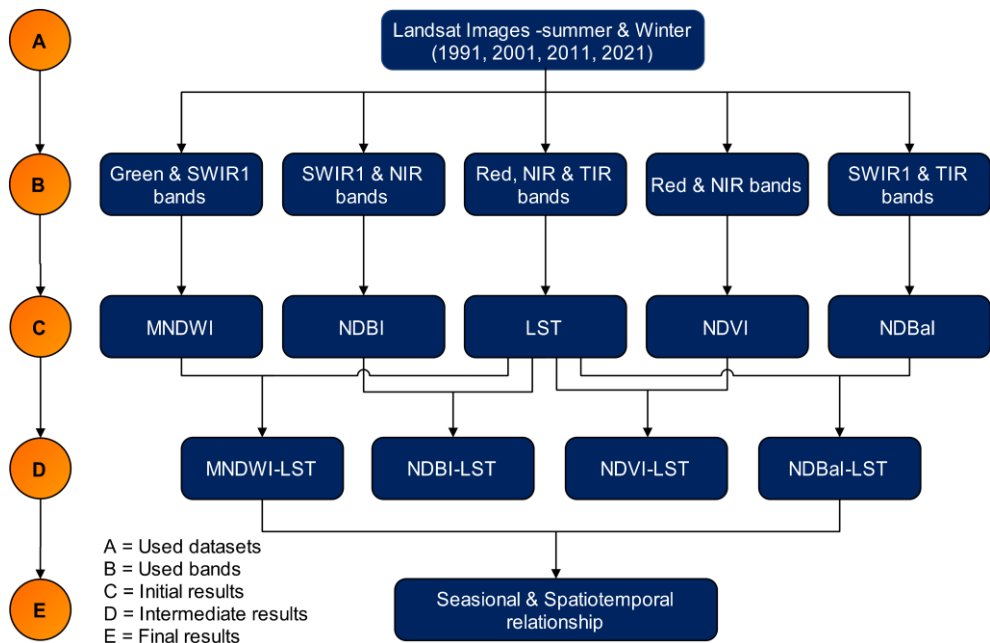
Finally, LST is computed by Eq. 5 (Weng *et al.*, 2004):

$$LST = \frac{T_B}{1 + (\lambda \sigma T_B / (hc)) \ln \mathcal{E}} \quad (5)$$

Where, λ = effective wavelength, σ = Boltzmann constant (1.38×10^{-23} J/K), h = Plank's constant (6.626×10^{-34} Js), C = velocity of light in a vacuum (2.998×10^8 m/sec), \mathcal{E} = emissivity.

The detailed picture of the methodology is shown by a flowchart in Figure 2:

Fig. 2: Flowchart showing the entire methodology of the present study



RESULTS

Changing status of LST

A significant spatial distribution of LST is observed from 1991 to 2021 with 10 years intervals (Figure 3). A gradual rise is observed in the mean, minimum, and maximum LST because of the variety of land surface materials. The forest and water areas declined whereas the settlement increased and this change of LULC is reflected in the distribution of LST. Northeast and central parts of Imphal obtain more LST every successive decade. In the winter season, the whole study area becomes hotter except in some parts of the north-western sides. The core part of the city is constantly getting warmed due to a fast rate of urbanization and land conversion.

Fig. 3: Spatial distribution of LST

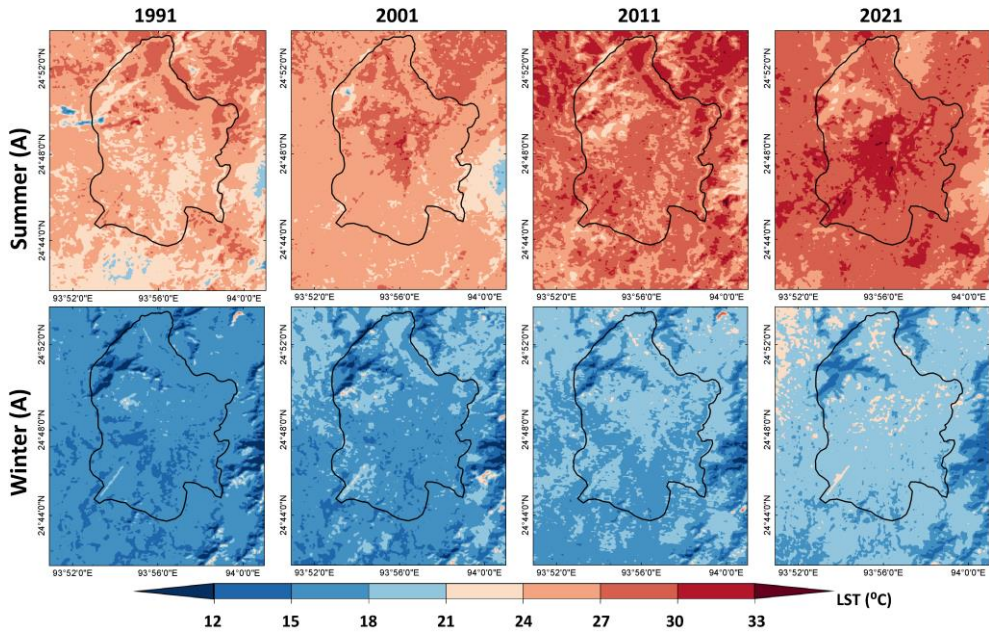


Table 3: Year-wise distribution and decadal change of LST (°C)

Temporal distribution			
Summer			
Year	LST(Min)	LST(Max)	LST(Mean)
1991	13.31	32.47	24.80
2001	17.02	32.05	25.59
2011	20.62	35.26	27.77
2021	21.66	34.75	28.37
Winter			
Year	LST(Min)	LST(Max)	LST(Mean)
1991	8.01	27.95	15.71
2001	9.97	30.44	19.09
2011	9.39	27.08	17.80
2021	11.39	30.36	18.80
Decadal change			
Summer			
Year	LST(Min)	LST(Max)	LST(Mean)
1991-2001	3.71	-0.42	0.79
2001-2011	3.60	3.21	2.18
2011-2021	1.04	-0.51	0.60
1991-2021	8.35	2.28	3.57
Winter			
Year	LST(Min)	LST(Max)	LST(Mean)
1991-2001	1.96	2.49	3.38
2001-2011	-0.58	-3.36	-2.29
2011-2021	2.00	2.28	1.10
1991-2021	3.38	2.41	3.09

Table 3 presents the year-wise LST distribution and decadal changes of LST in Imphal city for the entire period. The table shows that in summer, the minimum LST increases by 8.35 °C (from 13.31 °C to 21.66 °C), and in winter, it increases by 3.38 °C (from 8.01 °C to 11.39 °C). The maximum LST increases 2.28 °C (from 32.47 °C to 34.75 °C) in summer and 2.41 °C (from 27.95 °C to 30.36 °C) in winter. The mean LST increases 3.57 °C (from 24.80 °C to 28.37 °C) in summer and 3.09 °C (from 15.71 °C to 18.80 °C) in winter. Hence, LST substantially raises from the earlier decade to the next decade. In the meantime, the built-up area increases more than any other land use type, and forest area declines the most among the different land use types.

Seasonal and spatiotemporal status of four indices

Figures 4 and 5 show the spatial values of NDVI and MNDWI for summer and winter. Northern and eastern parts indicate a thick cover of natural vegetation. The summer image presents the true picture of the change in NDVI value. In 1991, the NDVI value was much higher than in 2001. 2001 image has more NDVI value than 2011 and obviously, the 2021 image indicates the lowest NDVI value among the four years. Apart from the loss of vegetation, greenness has also declined. It indicates that the dense forests become sparse and the nature of trees is also being changed. In the winter season, the NDVI values remain more constant. Moreover, agricultural activities can be considered as one of the controlling factors for the differences in NDVI values between the summer and winter. Several sizes of water bodies are developed in the eastern, north-central, and south-western portions of the having higher MNDWI values. The water surface area in the city remains almost the same during the period. Some water bodies have been developed along the eastern side of the study area and it is clearly shown in the 2021 image. The central part of the city has a moderate value of MNDWI.

Fig. 4: Spatial distribution of NDVI

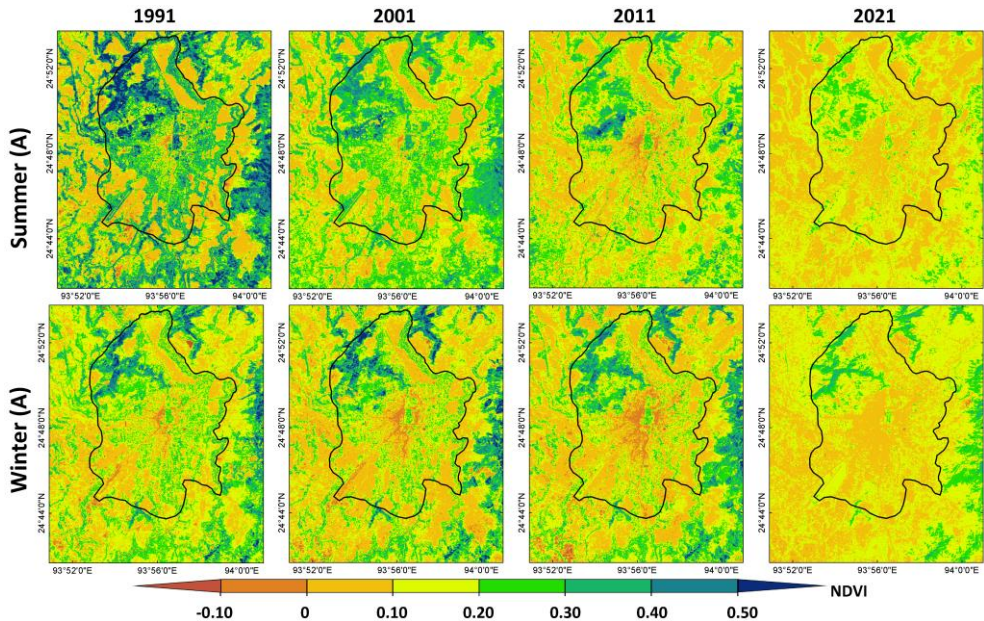


Fig. 5: Spatial distribution of MNDWI

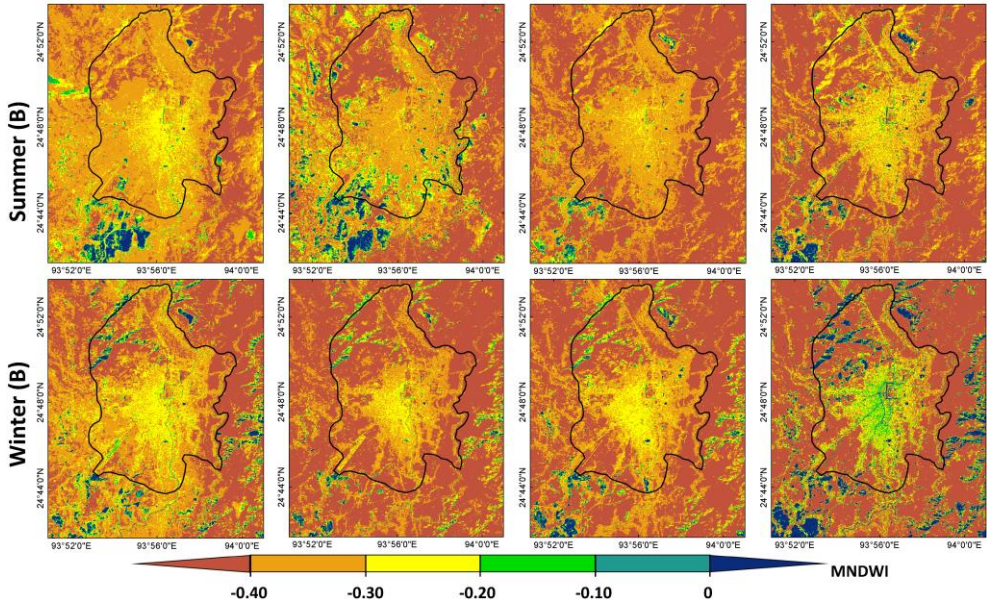


Fig. 6: Spatial distribution of NDBI

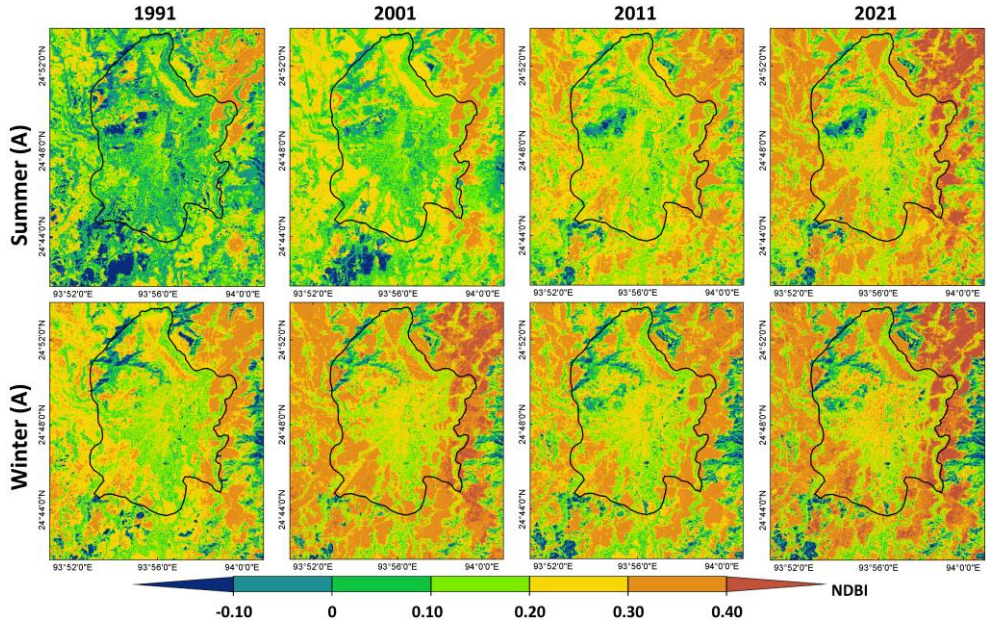
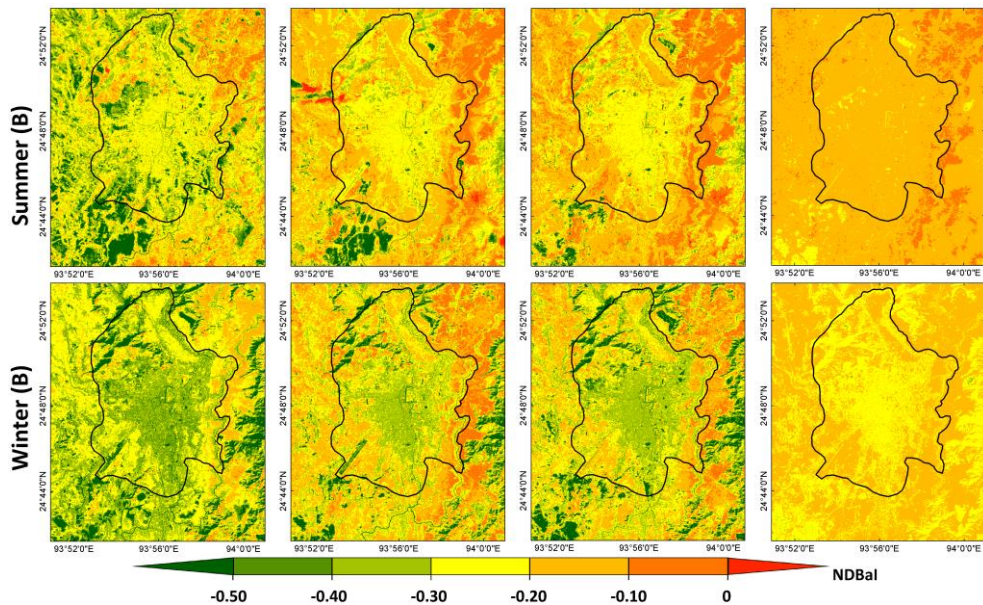


Fig. 7: Spatial distribution of NDBaI



Figures 6 and 7 show the spatial distribution (1991-2021) of NDBI. and NDBaI for the two seasons. In both seasons, NDBI values are constantly rising. NDBI values are higher in the inner and outer peripheries of the core city. However, in 2021, the central part also shows a high NDBI value. Winter images show higher NDBI than the summer. From 1991 to 2021, the NDBaI values increase rapidly. Except for the central part of the study area, every corner witnesses a high NDBaI value. This is due to higher vegetation and water coverage in the middle part of the core city. A very high NDBaI value is observed along the outskirts of the city where the soil is dry and the land is comparatively bare.

Figure 8 shows the scatter plots of NDVI with LST in summer and winter. The relationship is moderate negative throughout the study period. Generally, the summer season ($R = -0.39, -0.25, -0.61, \text{ and } -0.54$ for 1991, 2001, 2011, and 2021, respectively) has a slightly better correlation compared to winter ($R = -0.21, -0.42, -0.46, \text{ and } -0.48$ for 1991, 2001, 2011, and 2021, respectively). During the summer, the chlorophyll content in vegetation is much higher than in the winter season and it directly has an impact on the NDVI-LST relationship. Moreover, the strength of the negative relationship is continuously increasing during the winter, but it shows a neutral appearance in summer.

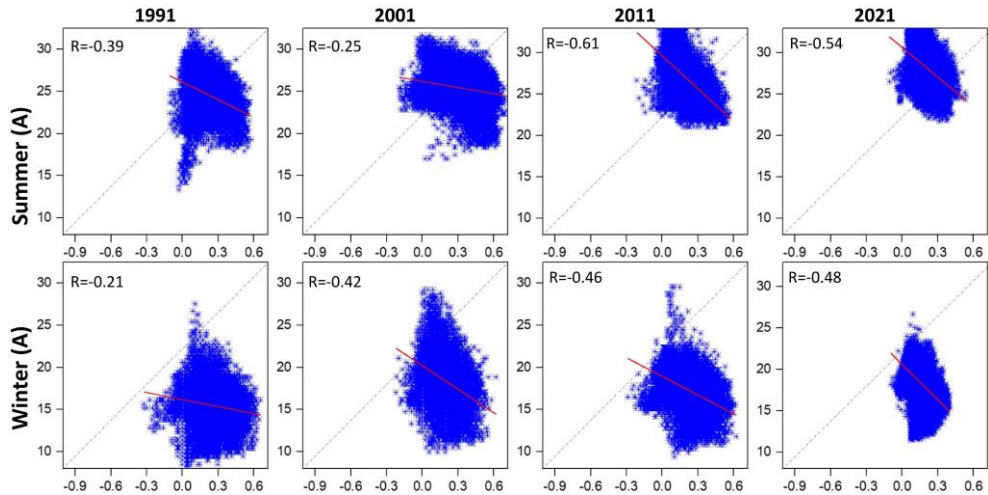
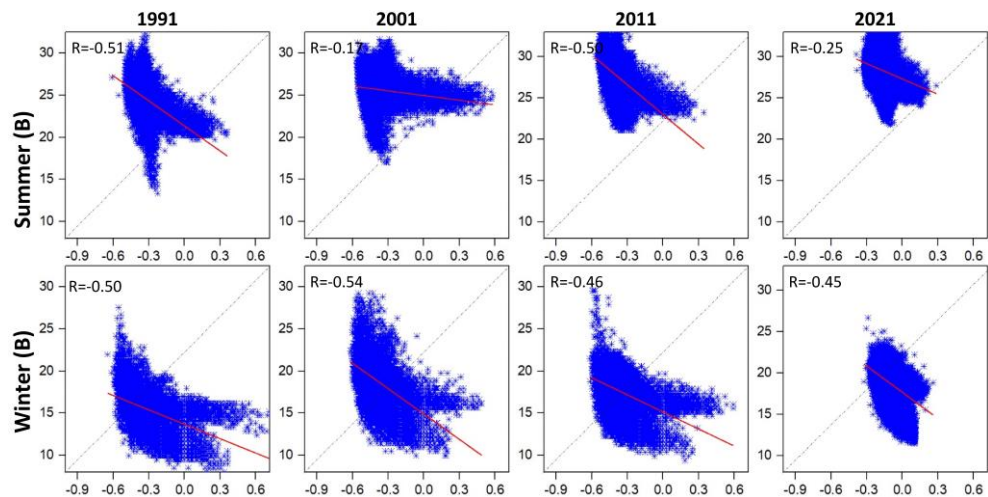
Fig. 8: Scatter plots of NDVI (x-axis) against LST (y-axis)**Fig. 9: Scatter plots of MNDWI (x-axis) against LST (y-axis)**

Figure 9 shows the scatter plots of MNDWI with LST for both seasons of the study span. It shows an inverse relationship with moderate strength for all eight images. However, the seasonal effect on the MNDWI-LST relationship is fluctuating in the summer season ($R = -0.51, -0.17, -0.50,$ and -0.25 for 1991, 2001, 2011, and 2021, respectively). This is mainly because of the fluctuation of moisture content in the air, wind speed, and evaporation rate. Winter season reflects a steady moderate inverse relationship ($R = -0.50, -0.54, -0.46,$ and -0.45 for 1991, 2001, 2011, and 2021, respectively). The negativity trend remains almost constant in winter. However, it has no such significant effect in the summer season.

Figure 10 shows the scatter plots of NDBI with LST in summer and winter for the study period. The relationship is moderate positive throughout the study period. The winter season ($R = 0.53, 0.67, 0.66,$ and 0.69 for 1991, 2001, 2011, and 2021, respectively) indicates a more stable NDBI-LST relationship than the summer ($R = 0.68, 0.38, 0.76,$ and 0.56 for 1991,

2001, 2011, and 2021, respectively). It means that despite the growth of population and settlement the road and building materials and conditions are not so much changed. The strength of the relationship is constantly rising in the winter season while it has almost no effect in the summer.

Fig. 10: Scatter plots of NDBI (x-axis) against LST (y-axis)

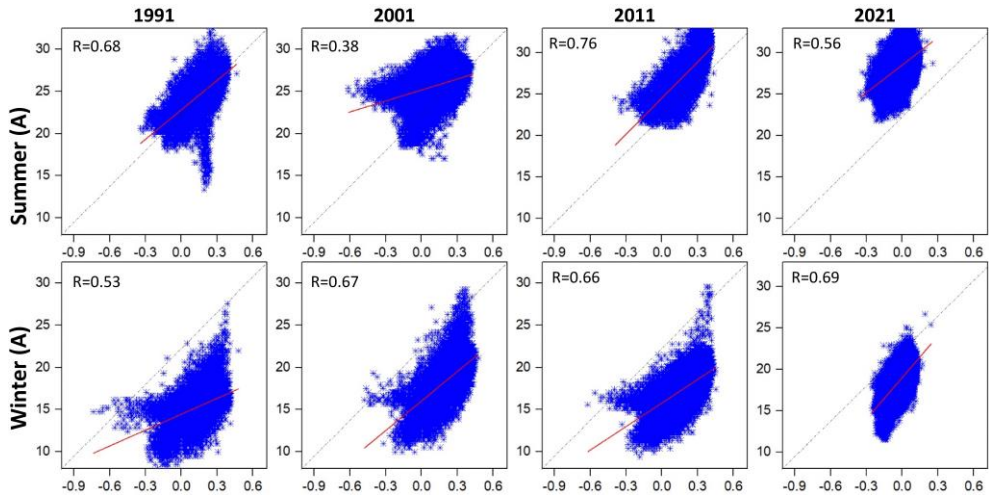


Fig. 11: Scatter plots of NDBaI (x-axis) against LST (y-axis)

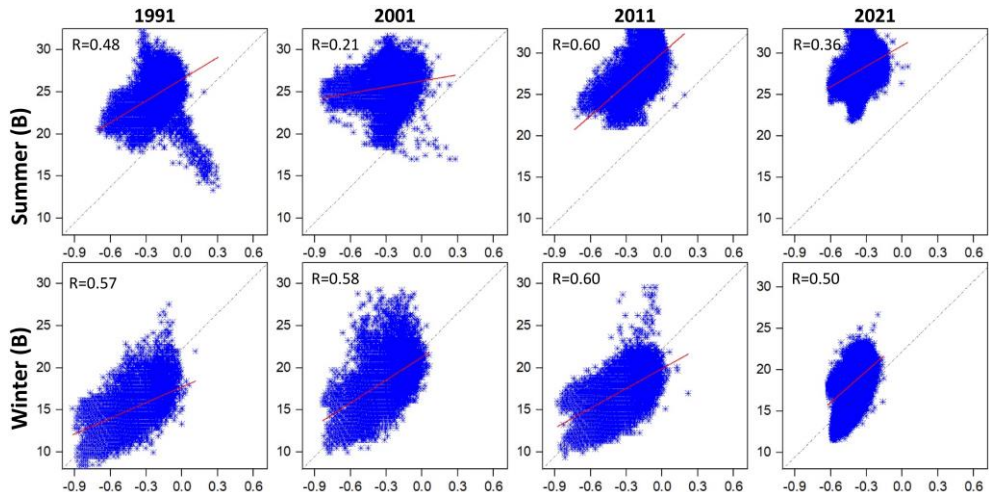


Figure 11 shows the scatter plots of NDBaI with LST in summer and winter from 1991 to 2021. It shows a moderate positive relationship. However, the seasonal effect on the NDBaI-LST relationship is more fluctuating in summer season ($R = 0.48, 0.21, 0.60,$ and 0.36 for 1991, 2001, 2011, and 2021, respectively). Condition and coverage of fallow land

and dry soil are varying and are irregular during the summer season. However, the winter season indicates a very stable moderate positive relationship ($R = 0.57, 0.58, 0.60,$ and 0.50 for 1991, 2001, 2011, and 2021, respectively). It happens due to the dryness of the area during this season. The strength of the relationship is slightly increasing in the winter season. However, the summer season reflects an irregular trend.

The results also show that all the relationships are more consistent in the winter season (values of the coefficient of variation are 7.31, 7.04, 10.45, and 28.71 for MNDWI, NDBaI, NDBI, and NDVI) than in summer (values of the coefficient of variation are 44.46, 36.09, 23.67, and 29.71 for MNDWI, NDBaI, NDBI, and NDVI). Moreover, among the spectral indices, NDBI builds the most consistent ($CV=18.19$) relationship with LST while NDVI builds the most variable ($CV = 30.37$) relationship.

DISCUSSION

Results of the entire study show that each of the four spectral indices is comfortably related to LST and it is explicitly expressed in both summer and winter seasons. These correlations between LST and spectral indices indicate that the variation of LST primarily depends upon the land surface materials which can be extracted from the spectral indices. The moderate positive relationship of LST with NDBI and NDBaI supports the results found in the earlier studies. Similarly, the moderate negative relationship of LST with NDVI and MNDWI also supports the earlier observed results.

Liang *et al.* (2012) and Guha *et al.* (2022) observed a negative NDVI-LST correlation. Again, Yue *et al.* (2007) showed that the LST-NDVI relationship in Shanghai City, China was negative and was highly dependent on LULC types. Sun & Kafatos (2007) stated that this correlation was negative in the summer season. This relationship was also negative in Mashhad, Iran (Gorgani *et al.*, 2013). The relationship was strongly negative in Berlin City irrespective of any season (Marzban *et al.* 2018). This correlation tends to be more negative with the increase in surface moisture (Prehodko & Goward, 1997). The current study on Imphal also indicates the negative status of LST-NDVI correlation for summer (average correlation coefficient is -0.45) and winter (average correlation coefficient is -0.39). The value of the correlation coefficient is inversely related to the surface moisture content, i.e., the negativity of the relationship increases with the increase of surface moisture content.

The LST-NDBI correlation found in the current study is stable and moderately positive in both seasons (the average correlation coefficient during summer is 0.64 and during winter is 0.60) for the entire period of study. This result significantly supports many other earlier LST-NDBI related research works performed in Fuzhou City, China (Zhang *et al.*, 2009), Bahir Dar City, Ethiopia (Balew and Korme 2020), Melbourne City, Australia (Jamei *et al.*, 2019), Metropolitan Area of Bangladesh (Roy *et al.*, 2020), San Salvador City, El Salvador (Son *et al.*, 2020), Kunming, China (Chen & Zhang, 2017), Wuhan City, China (Chen *et al.*, 2013).

LST built a moderate negative relation with MNDWI for summer (average correlation coefficient is -0.36) and winter (average correlation coefficient is -0.49) throughout the study. It signifies past research works. Ma & Peng (2022) showed that LST correlates moderately negative (-0.63) with MNDWI in Kunming, China. The relationship was negative in Sepidan County, Iran (Taripanah & Ranjbar 2021). Guha & Govil (2021) also showed that LST and MNDWI built a negative correlation in Raipur, India. Moreover, Mashiella *et al.* (2020) established that LST builds a strong negative (-0.78) relation with MNDWI in Sleman Regency, Indonesia.

The current study indicates that LST builds a moderate positive correlation (average correlation coefficient during summer is 0.41 and during winter is 0.56) with NDBaI in Imphal City, India. This research output reflects similar nature to the previous works. Essa *et al* (2012) also showed a moderate positive LST-NDBaI correlation (0.39) in the Greater Dublin region, Ireland. A strong positive LST-NDBaI relationship was also observed in Kunming, China (Chen and Zhang 2017). LST and NDBaI built a weak positive correlation in London and Baghdad (Ali *et al.*, 2017). Nimish *et al.* (2020) investigated a positive ($R^2=0.21$) relationship in Kolkata, India. This correlation was weak and positive (0.06) in Harare, Zimbabwe (Mushore *et al.*, 2017). In the National Capital Region of India, the relationship was moderate positive (Sharma and Joshi 2016).

The study reflects the scenario of LST change and variation of the relationship of LST with the four spectral indices. Moreover, NDBaI extracts bare land, NDBI extracts built-up area, NDVI extracts green vegetation and MNDWI extracts water bodies with wetlands. As these four indices help in delineating various types of land use, the landscape ecology of the city significantly depends on the values of these indices. The low LST zones are certainly found in the forest or wetlands or water bodies (areas with high NDVI or high MNDWI values) whereas the high LST values generate in the built-up surface and barren land surface (areas with high NDBI or high NDBaI values). If the barren or fallow lands are converted into green or water areas, the ecology of the city will be healthier. Thus, urban planners should follow the basic conversion of the city so that the landscape ecology of the city becomes environmentally rich.

Conclusion

The paper evaluates the seasonal and spatiotemporal relation of LST with MNDWI, NDVI, NDBaI, and NDBI using multi-temporal Landsat satellite images in and around Imphal city. During the whole span, LST raises at 14.39 % decadal rate in summer and at 19.67 % decadal rate in winter. The central part of the city is the most heated part due to the high concentration of commercial and industrial infrastructure.

Furthermore, the relationships of LST with these spectral indices were quantified. For the whole study area in the last thirty years, NDVI and MNDWI build a moderate negative relation with LST; NDBI and NDBaI build a moderate positive relation with LST. These relationships are more consistent in the winter season than in summer. The negativity trend is gradually increasing for the NDVI-LST relationship in the winter season, but in summer it is fluctuating. The negativity trend is slightly decreasing for the MNDWI-LST relationship in winter, but in summer there is no such type of increasing or decreasing trend has been noticed. In winter, the positivity trend of the NDBI-LST relationship is rising gradually, but the trend is fluctuating in summer. In the case of the NDBaI-LST relationship, the positivity trend is also slightly increasing in winter, but the trend is irregular in summer. The results indicate that the variability of the spectral indices-LST relationship is more in the summer season due to the high variability of moisture content in the air. Regarding consistency among the all the spectral indices, NDBI is considered the most reliable while NDVI is considered the most variable index.

ACKNOWLEDGMENT

The authors are indebted to United States Geological Survey (USGS), Imphal Municipal Corporation (IMC), and Google Earth.

CONFLICTS OF INTEREST

The authors declare no conflict of interest

REFERENCES

- Ali, J.M., Marsh, S.H., Smith, M.J. (2017). A comparison between London and Baghdad surface urban heat islands and possible engineering mitigation solutions. *Sustain Cities Soc* 29: 159-168. <https://doi.org/10.1016/j.scs.2016.12.010>
- Arnfield, J. (2003). Two decades of urban climate research: a review of turbulence, exchanges of energy and water, and the urban heat island. *Int J Climatol* 23: 1–26. <https://doi.org/10.1002/joc.859>
- Artis, D.A., Carnahan, W.H. (1982). Survey of emissivity variability in thermography of urban areas. *Remote Sens Environ* 12(4), 313–329.
- Balew, A., Korme, T. (2020). Monitoring land surface temperature in Bahir Dar city and its surrounding using Landsat images. *Egypt J Remote Sens Space Sci* <https://doi.org/10.1016/j.ejrs.2020.02.001>
- Carlson, T.N., Ripley, D.A. (1997). On the Relation between NDVI, Fractional Vegetation Cover, and Leaf Area Index. *Remote Sens Environ* 62: 241-252. [https://doi.org/10.1016/S0034-4257\(97\)00104-1](https://doi.org/10.1016/S0034-4257(97)00104-1)
- Chen, L., Li, M., Huang, F., Xu, S. (2013). Relationships of LST to NDBI and NDVI in Wuhan City based on Landsat ETM+ image. In *6th International Congress on Image and Signal Processing (CISP)* (pp. 840-845), Hangzhou, 2013.
- Chen, X.L., Zhao, H.M., Li, P.X., Yi, Z.Y. (2006). Remote sensing image-based analysis of the relationship between urban heat island and land use/cover changes. *Remote Sens Environ* 104(2): 133–146. <https://doi.org/10.1016/j.rse.2005.11.016>
- Chen, X., Zhang, Y. (2017). Impacts of urban surface characteristics on spatiotemporal pattern of land surface temperature in Kunming of China. *Sustain Cities Soc.* 32: 87-99. <https://doi.org/10.1016/j.scs.2017.03.013>
- Deilami, K., Kamruzzaman, M., Liu, Y. (2018). Urban heat island effect: A systematic review of spatio-temporal factors, data, methods, and mitigation measures. *Int J Appl Earth Obs Geoinf* 67: 30-42. <https://doi.org/10.1016/j.jag.2017.12.009>
- Equere, V., Mirzaei, P.A., Riffat, S. (2020). Definition of a new morphological parameter to improve prediction of urban heat island. *Sustain Cities Soc* 56: 102021. <https://doi.org/10.1016/j.scs.2020.102021>
- Essa, W., Verbeiren, B., Van der Kwast, J., Van de Voorde, T., Batelaan, O. (2012).. Evaluation of the DisTrad thermal sharpening methodology for urban areas. *Int J Appl Earth Obs Geoinf* 19: 163-172. <https://doi.org/10.1016/j.jag.2012.05.010>
- Feng, Y., Li, H., Tong, X., Chen, L., Liu, Y. (2018). Projection of land surface temperature considering the effects of future land change in the Taihu Lake Basin of China. *Global Planet Change* 167: 24-34. <https://doi.org/10.1016/j.gloplacha.2018.05.007>
- Ferrelli, F., Huamantincó, M.A., Delgado, D.A., Piccolo, M.C. (2018). Spatial and temporal analysis of the LST-NDVI relationship for the study of land cover changes and their contribution to urban planning in Monte Hermoso, Argentina. *Doc Anal Geogr* 64 (1): 25-47. <https://doi.org/10.5565/rev/dag.355>
- Feyisa, G.L., Meilby, H., Jenerette, G.D., Pauliet, S. (2016). Locally optimized separability

enhancement indices for urban land cover mapping: Exploring thermal environmental consequences of rapid urbanization in Addis Ababa, Ethiopia. *Remote Sens Environ* 175: 14-31. <https://doi.org/10.1016/j.rse.2015.12.026>

Filho, WLFC, De Barros, Santiago, D., De Oliveira-Júnior, J.F., Da Silva Junior, C.A. (2019). Impact of urban decadal advance on land use and land cover and surface temperature in the city of Maceió, Brazil. *Land Use Policy* 87: 104026. <https://doi.org/10.1016/j.landusepol.2019.104026>

Gorgani, S.A., Panahi, M., Rezaie, F. (2013). *The relationship between NDVI and LST in the Urban area of Mashhad, Iran*. International Conference on Civil Engineering Architecture and Urban Sustainable Development. November, Tabriz, Iran.

Guha, S., Govil, H. (2021). Annual assessment on the relationship between land surface temperature and six remote sensing indices using Landsat data from 1988 to 2019. *Geocarto International*. <https://doi.org/10.1080/10106049.2021.1886339>

Guha, S., Govil, H., Mukherjee, S. (2017). Dynamic analysis and ecological evaluation of urban heat islands in Raipur city, India. *Journal of Applied Remote Sensing*. 11(3): 036020. <https://doi.org/10.1117/1.JRS.11.036020>

Guha, S., Govil, H., Taloor, A.K., Gill, N., Dey, A. (2022). Land surface temperature and spectral indices: A seasonal study of Raipur City. *Geodesy and Geodynamics*. 13(1): 72-82. <https://doi.org/10.1016/j.geog.2021.05.002>

Jamei, Y., Rajagopalan, P., Sun, Q.C. (2019). Spatial structure of surface urban heat island and its relationship with vegetation and built-up areas in Melbourne, Australia. *Sci Total Environ* 659: 1335-1351. <https://doi.org/10.1016/j.scitotenv.2018.12.308>

Kalota, D. (2017). Exploring relation of land surface temperature with selected variables using geographically weighted regression and ordinary least square methods in Manipur State, India. *Geocarto Int* 32(10): 1105-1119. <https://doi.org/10.1080/10106049.2016.1195883>

Liang, B.P., Li, Y., Chen, K.Z. (2012). A Research on Land Features and Correlation between NDVI and Land Surface Temperature in Guilin City. *Remote Sens Tech Appl* 27: 429-435.

Li, J., Song, C., Cao, L., Meng, X., Wu, J. (2011). Impacts of landscape structure on surface urban heat islands: A case study of Shanghai, China. *Remote Sens Environ* 115: 3249-3263.

Lopez, J.M.R., Heider, K., Scheffran, J. (2017). Frontiers of urbanization: Identifying and explaining urbanization hot spots in the south of Mexico City using human and remote sensing. *Appl Geogr* 79: 1-10.

Ma, X., Peng, S. (2022). Research on the spatiotemporal coupling relationships between land use/land cover compositions or patterns and the surface urban heat island effect. *Environ Sci Pollut Res Int* 29(26): 39723-39742. <https://doi.org/10.1007/s11356-022-18838-3>

Maishella, A., Dewantoro, B.E.B., Aji, M.A.P. (2018). Correlation Analysis of Urban Development and Land Surface Temperature Using Google Earth Engine in Sleman Regency, Indonesia. IOP Conf. Series: *Earth and Environmental Science* 540 (2020) 012018. <https://doi.org/10.1088/1755-1315/540/1/012018>

Marzban, F., Sodoudi, S., Preusker, R. (2018). The influence of land-cover type on the relationship between LST-NDVI and LST-Tair. *Int J Remote Sens* 39(5): 1377-1398. <https://doi.org/10.1080/01431161.2017.1462386>

Mirzaei, P.A. (2015). Recent challenges in modeling of urban heat island. *Sustain Cities Soc*

19: 200–206. <https://doi.org/10.1016/j.scs.2015.04.001>

Mondal, A., Guha, S., Kundu, S. (2021). Dynamic status of land surface temperature and spectral indices in Imphal city, India from 1991 to 2021. *Geomatics, Natural Hazards and Risk*. 12(1): 3265–3286. <https://doi.org/10.1080/19475705.2021.2008023>

Mushore, T.D., Odindi, J., Dube, T., Matongera, T.N., Mutangam, O. (2017). Remote sensing applications in monitoring urban growth impacts on in-and-out door thermal conditions: A review. *Remote Sens Appl Soc Environ* 8: 83–93. <https://doi.org/10.1016/j.rsase.2017.08.001>

Nie, Q., Man, W., Li, Z., Huang, Y. (2016). Spatiotemporal Impact of Urban Impervious Surface on Land Surface Temperature in Shanghai, China. *Can J Remote Sens* 42(6): 680–689. <http://dx.doi.org/10.1080/07038992.2016.1217484>

Nimish, G., Bharath, H.A., Lalitha, A. (2020). Exploring temperature indices by deriving relationship between land surface temperature and urban landscape. *Remote Sens Appl Soc Environ* 18: 100299. <https://doi.org/10.1016/j.rsase.2020.100299>

Pearsall, H. (2017). Staying cool in the compact city: Vacant land and urban heating in Philadelphia, Pennsylvania. *Appl Geogr* 79: 84–92. <http://dx.doi.org/10.1016/j.apgeop.2016.12.010>

Peng, J., Xie, P., Liu, Y., Ma, J. (2016). Urban Thermal Environment Dynamics and Associated Landscape Pattern Factors: A Case Study in the Beijing Metropolitan Region. *Remote Sens Environ* 173: 145–155.

Prehodko, L., Goward, S.N. (1997). Estimation of Air Temperature from Remotely Sensed Surface Observations. *Remote Sens Environ* 60: 335–346. [https://doi:10.1016/S0034-4257\(96\)00216-7](https://doi:10.1016/S0034-4257(96)00216-7)

Rinner, C., Hussain, M. (2011). Toronto's urban heat island exploring the relationship between land use and surface temperature. *Remote Sens* 3: 1251–1265. <https://doi.org/10.3390/rs3061251>

Rizwan, A.M., Dennis, L.Y.C., Liu, C. (2008). A review on the generation, determination and mitigation of Urban Heat Island. *J Environ Sci* 20: 120–128.

Roy, S., Pandit, S., Eva, E.A., Bagmar, M.S.H., Papia, M., Banik, L., Dube, T., Rahman, F., Razi, M.A. (2020). Examining the nexus between land surface temperature and urban growth in Chattogram Metropolitan Area of Bangladesh using long term Landsat series data. *Urban Clim* 32: 100593. <https://doi.org/10.1016/j.uclim.2020.100593>

Sharma, R., Joshi, P.K. (2016). Mapping environmental impacts of rapid urbanization in the National Capital Region of India using remote sensing inputs. *Urban Clim* 15: 70–82. <https://doi.org/10.1016/j.uclim.2016.01.004>

Sobrino, J.A., Raissouni, N., Li, Z. (2001). A comparative study of land surface emissivity retrieval from NOAA data. *Remote Sens Environ* 75(2): 256–266. [https://doi.org/10.1016/S0034-4257\(00\)00171-1](https://doi.org/10.1016/S0034-4257(00)00171-1)

Sobrino, J.A., Jimenez-Munoz, J.C., Paolini, L. (2004). Land surface temperature retrieval from Landsat TM5. *Remote Sens Environ* 9: 434–440. <https://doi:10.1016/j.rse.2004.02.003>

Song, X., Hansen, M.C., Stehman, S.V., Potapov, P.V., Tyunkvina, A., Vermote, E.F., Townshend, J.R. (2018). Global land change from 1982 to 2016. *Nature* 560: 639–643. <https://doi: 10.1038/s41586-018-0411-9>

Son, N.T., Chen, C.F., Chen, C.R. (2020). Urban expansion and its impacts on local temperature in San Salvador, El Salvador. *Urban Clim* 32: 100617.

<https://doi.org/10.1016/j.uclim.2020.100617>

Son, Y.S., Kang, M.K., Yoon, W.J. (2014). Lithological and mineralogical survey of the Oyu Tolgoi region, South-eastern Gobi, Mongolia using ASTER reflectance and emissivity data. *Int J Appl Earth Obs Geoinf* 26: 205–216.

Song, J., Du, S., Feng, X., Guo, L. (2014). The Relationships Between Landscape Compositions and Land Surface Temperature: Quantifying Their Resolution Sensitivity With Spatial Correlation Models. *Landsc Urban Plan* 123: 145–157.

Sun, D., Kafatos, M. (2007). Note on the NDVI-LST Relationship and the Use of Temperature-Related Drought Indices over North America. *Geophys Res Lett* 34. <http://doi:10.1029/2007GL031485>

Taripana, F., Ranjbar, A. (2021). Quantitative analysis of spatial distribution of land surface temperature (LST) in relation to Ecohydrological, terrain and socio-economic factors based on Landsat data in mountainous area. *Adv Space Res* 68(9): 3622-3640. <https://doi.org/10.1016/j.asr.2021.07.008>

Tucker, C.J. (1979). Red and photographic infrared linear combinations for monitoring vegetation. *Remote Sens Environ* 8(2): 127–150.

Weng, Q.H., Lu, D.S., Schubring, J. (2004). Estimation of Land Surface Temperature–Vegetation Abundance Relationship for Urban Heat Island Studies. *Remote Sens Environ* 89: 467-483. <https://doi:10.1016/j.rse.2003.11.005>

Xu, H. (2006). Modification of normalized difference water index (NDWI) to enhance open water features in remotely sensed imagery. *Int J Remote Sens* 27(14): 3025–3033.

Yue, W., Xu, J., Tan, W., Xu, L. (2007). The Relationship between Land Surface Temperature and NDVI with Remote Sensing. Application to Shanghai Landsat 7 ETM+ data. *Int J Remote Sens* 28: 3205–3226. <https://doi.org/10.1080/01431160500306906>

Zhang, Y., Odeh, I.O.A., Han, C. (2009). Bi-temporal characterization of land surface temperature in relation to impervious surface area, NDVI and NDBI, using a sub-pixel image analysis. *Int J Appl Earth Obs Geoinf* 11(4): 256-264. <https://doi.org/10.1016/j.jag.2009.03.001>

Zhao, H.M., Chen, X.L. (2005). Use of normalized difference bareness index in quickly mapping bare areas from TM/ETM+. *Geoscience and Remote Sensing Symposium*, 3(25–29): 1666–1668. <https://doi.org/10.1109/IGARSS.2005.1526319>

Zhao, M., Cai, H., Qiao, Z., Xu, X. (2016). Influence of urban expansion on the urban heat island effect in Shanghai. *Int J Geogr Inf Sci* 30(12): 2421–2441. <https://doi.org/10.1080/13658816.2016.1178389>

Zha, Y., Gao, J., Ni, S. (2003). Use of normalized difference built-up index in automatically mapping urban areas from TM imagery. *Int J Remote Sens* 24(3): 583-594. <https://doi.org/10.1080/01431160304987>

Website: <http://earthexplorer.usgs.gov/>

<https://earth.google.com/web/>

<https://imc.mn.gov.in/>